JCTC Journal of Chemical Theory and Computation

Structure, Binding Energies, and IR-Spectral Fingerprinting of Formic Acid Dimers

İlhan Yavuz

Physics Department, Marmara University, Göztepe Kampus, Kadiköy 34772, Istanbul, Turkey

Carl Trindle*

Chemistry Department, The University of Virginia, Charlottesville, Virginia 22904

Abstract: We describe equilibrium structures for a variety of species likely to be formed as intermediate species in the dimerization of formic acid to produce the stable C_{2h}-symmetric doubly H-bonded dimer and perhaps produced as the vapor is irradiated. For several low-lying species the rearrangement pathways to the stable form are characterized at the MP2/6-311+G-(d,p) level of theory, with optimized structures and vibrations computed with full counterpoise corrections for basis set superposition error. Estimates of vibrational frequencies with corrections for anharmonicity suggest that infrared transitions (CO stretches and OH out-of-plane motions) could signal the presence of species less stable than the C_{2h} dimer, observable in irradiation studies of formic acid vapor.

Introduction

Formic acid **I** exists primarily as the trans form (the H−C−O−H angle = 180) in the gas phase. The MP2/6-311+G-(d,p) energy difference of 4.65 kcal/mol (4.40 kcal/mol after zero point energy correction[1,2]) suggests that the trans[3] form is about 1000× more abundant than the cis form at room temperature.

I-trans   **I**-cis
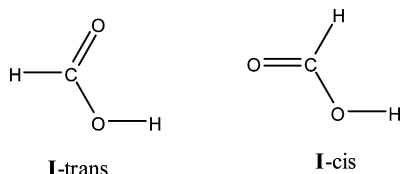
Formic acid forms clusters in the gas phase. The structure and spectra of the C_{2h}-symmetric dimer of formic acid **II** (below) has been thoroughly studied, both by computational modeling[4] and by spectroscopic methods.[5] Considerable emphasis has been placed on the proton exchange and the importance of tunneling in the process.[6]

Shipman et al.[7] have investigated the response of formic acid vapor to IR irradiation in the broad absorption associated with the OH stretch. The breadth has been rationalized by anharmonic coupling to lower-frequency modes, Fermi resonance with combinations of such modes, and (in the case of the symmetric dimer) Davydov coupling between the degenerate OH stretches. Low-temperature studies and temperature-dependent FTIR investigations have provided the basis for the study of intramolecular vibrational relaxation. The studies of Shipman et al. characterize vibrational relaxation of formic acid vapor near room temperature, subjected to an ultrashort (ca. 100 fs) pulse in the OH stretching region. Their observations suggest H-bond breaking with a characteristic time of about 20 ps and perhaps the existence of detectable amounts of a dimer other than the most stable C_{2h} species. The feature associated with the possible new structure, which the authors term the "acyclic" dimer, is broad, centered at about 3230 cm^{-1}. This may be compared with the cyclic dimer's OH stretch at 3107 cm^{-1} and suggests weaker H-bonding in what might be a short-lived species. The broad feature evolves over a 100 to 200 ps duration. The authors consider the possibility that colli-

---

* Corresponding author e-mail: cot@virginia.edu.

Chart 1. Structures of Species Discussed in the Text
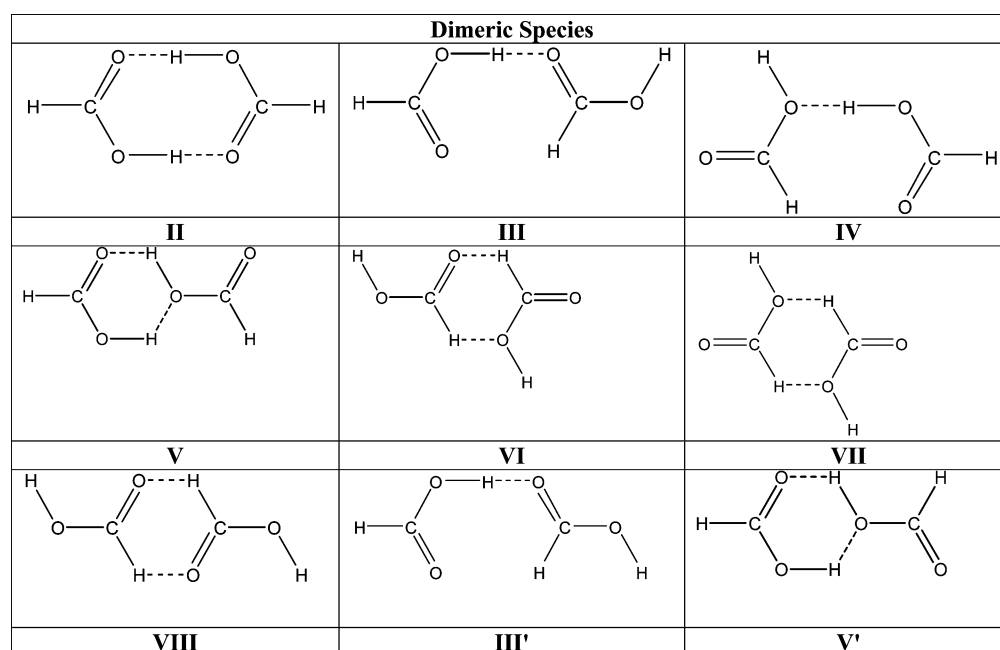
Chart 2. Energies (kcal/mol) Relative to Two Trans Formic Acid Molecules[a]
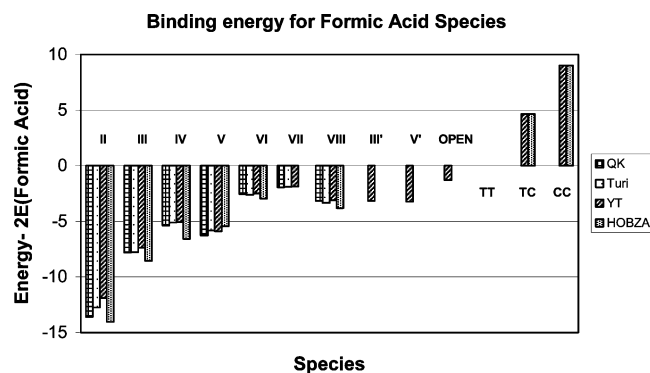
[a] Turi values from ref 8; QK values from Qian and Krim, ref 9; CVH values from Chocholoušová, Vacek, and Hobza, ref 10; YT=this work (Yavuz and Trindle). Turi and QK have single-point CP corrections; CVH and YT used full counterpoise corrections in optimization. ZPE corrections are not included. TT refers to two isolated formic acid molecules in trans configuration; TC and CC have one and two cis species respectively.

sional cooling of the acyclic dimer(s) may account for the longer-time behavior but concluded that the growth in free OH absorption could not be rationalized in this way. Their preferred account is a dissociation of an acyclic dimer to monomers in the 100 to 200 ps time frame. Direct dissociation requires 14.8 kcal/mol (or about 5000 cm^{-1}) according to photoacoustic measurement,[8] so the 3000 cm^{-1} provided by IR irradiation must be augmented, perhaps by collision.

The purpose of this investigation is to re-examine the energy demands for the formation of acyclic dimers and the further production of monomers for such intermediate species. We intend to identify species within the energy reach of the irradiation and to characterize their IR absorption spectra to provide a basis for more direct identification of the intermediate species. To this end we conduct computa-

tions employing correlation-corrected model chemistries (MP2 in extended basis sets), corrected by counterpoise compensation for Basis Set Superposition Errors and including estimates of anharmonicity and mode coupling.

Modeling such small interactions as hydrogen bonds requires accurate methods. This includes a suitably large and flexible basis set, recognition of correlation corrections to energies and structures, and allowance for basis set superposition error (BSSE).[9,10] According to Tzusuki et al.,[3] the extrapolated basis set limit for the counterpoise (CP)-corrected binding energy in CCSD(T) for the C_{2h}-symmetric dimer of formic acid is 13.93 kcal/mol. Their estimate of the MP2 limit for the binding energy is 13.79 kcal/mol. We infer that these values are not ZPE-corrected. The landmark paper of Turi[11] characterized this species and defined a standard notation for other equilibrium structures **II−VIII** of the dimers of *trans*-formic acid, using MP2 with basis sets up to D95++(d,p) and single-point counterpoise estimates of the basis set superposition error.

Among the dimers of trans formic acid we find conventional linear =O...HO− and >O...HO− hydrogen bonds (**II** in the first case, **III** and **IV** in the second case), bent -OH...O< H-bonds which are probably slightly weaker (**V** and **V′**), shared H bonds, and much weaker CH...O< and CH...O= interactions (**III**, **III′**, **IV**, **VI**, **VII**, **VIII**). The binding energy can be approximately represented by the energies of the various types of H-bonds: the weak interaction CH...O on average is about 1 kcal/mol; OH...O is about 5−6 kcal/mol; and the distorted bond OH...O is about 3 kcal/mol. Qian and Krimm[12] revisited these systems in their project to construct a suitable potential for molecular mechanics simulations. Their MP2/6-311++G(d,p) binding energies, counterpoise-corrected for BSSE at the equilibrium geometries, are in general agreement with Turi's results. Chocholoušová, Vacek, and Hobza[13] (CVH) have evaluated energies and structures of several of these species, with the MP2/aug-cc-pVDZ model chemistry including both

Table 1. New Equilibrium Structures and Energies Relative to Twice **I-trans** without and with Zero Point Energy Corrections (kcal/mol)
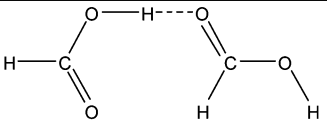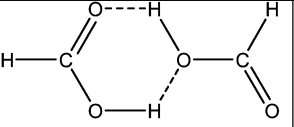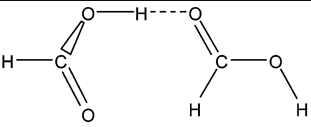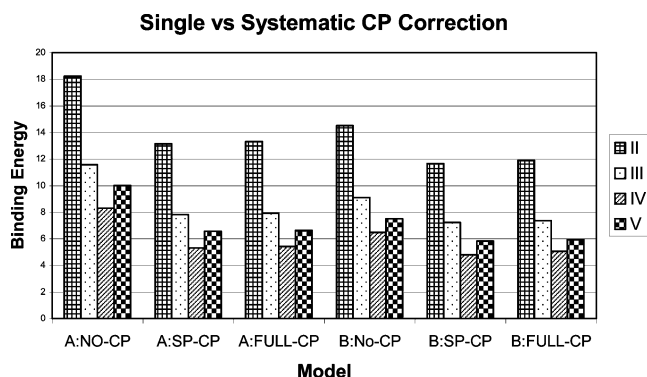
Code	III'	V'	Open
Form			
E	-3.15	-3.24	-1.38
E(ZPE)	-1.75	-2.10	-0.51

Chart 3. Counterpoise Corrections of Two Kinds, Single Point and Full[a]

Single vs Systematic CP Correction

[a] Binding energy estimates for species **II**, **III**, **IV**, and **V** for various counterpoise corrections. Region A: left to right, MP2/6-31G(d) values with no CP correction, single-point CP, or optimized on a fully CP-corrected surface. Region B: left to right, analogous MP2/6-311+G(d,p) values. All energies are in kcal/mol.

counterpoise-corrected optimization and single-point correction of the energy after conventional optimization. We have returned to these systems as the first step in a study of species that might be generated when formic acid vapor is irradiated by 3000 cm^{-1} photons.

All our calculations employ Gaussian 03(W).[14] In our best calculations our model chemistry is MP2/6-311+G(d,p) with full counterpoise corrections[7] imposed throughout the optimization and frequency calculations. By "full counterpoise corrections" we mean that the method of Simon, Duran, and Dannenberg is employed.[7] At every point in an optimization the energy and gradient E and ∇E are computed for the dimer FA−FA* (where FA and FA* are both formic acid molecules but may be differently disposed in space) in the joint basis BFA∪BFA*; for each monomer in the joint basis; and for each monomer in its own basis. Then the energy is written

$$E = E(\text{FA} + \text{FA*};\text{BFA} \cup \text{BFA*}) +$$
$$E(\text{FA};\text{BFA} \cup \text{BFA*}) + E(\text{FA*};\text{BFA} \cup \text{BFA*}) -$$
$$E(\text{FA*};\text{BFA*}) - E(\text{FA};\text{BFA})$$

The counterpoise-corrected gradient and second derivative tensor require the derivatives of all four correction terms as well as the leading term. Simon, Duran, and Dannenberg report several cases, notably HF in water, where full CP produces significantly different structures and vibrational frequencies compared with single point CP correction.

Chart 2 displays various estimates of the energies of the nine species identified by Turi,[8] relative to the dissociation products, two separated trans formic acid molecules. These values do not include zero-point energy corrections. We have interchanged species **IV** and **V** in CVH Table 1 (III and IV in their numbering), after reproducing their reported numbers for these species. It appears that values in the first column of CVH in Table 1 refer to binding energies obtained by conventional optimization followed by single-point counterpoise correction. Table S2 (Supporting Information) includes more detail of the results of Turi, Qian and Krimm, and Chocholoušová, Vacek, and Hobza as well as our own, including zero point energies and CP corrections. The key difference between our results and these values is the relative stability we find for species **V** which displays a −OH bond participating both as an acceptor and a donor in the six-atom ring stabilized by H bonds.

Brinkmann, Tschumper, Yan, and Schaeffer[15] have studied species **I**, **II**, and **III**, using a variety of basis sets and both MP2 and DFT correlation-corrected model chemistries. They estimate the binding energy of **II** to be about 15.9 kcal/mol (with MP2 with their TZ2P+dif basis) and of **III** to be about 9.5 kcal/mol. The counterpoise correction is about 2.4 kcal/mol for **II** and 0.6 kcal/mol for **III**; this would shift the binding energies of **II** and **III** to 13.5 and 8.9 kcal/mol respectively. These values are apparently not corrected for zero-point vibrational energy.

Our values seem to be consistent with Turi's values, but our binding energy values are smaller for species **II** and **III**. This may arise either from details of the counterpoise corrections or effects of the difference in basis used; we locate minimum-energy structures and vibrational frequencies on the counterpoise-corrected potential, while Qian and Krimm and also Turi evaluate the CP correction using structures obtained by direct calculations. Chocholoušová, Vacek, and Hobza report results of both single-point CP corrections and counterpoise-corrected optimization. In general one expects smaller binding energies and lower interfragment frequencies for the counterpoise-corrected optimization compared to standard gradient optimization.

Equilibrium structures found on the CP-corrected surfaces may be quite different in geometry and as well as energy relative to the analogous structures located on the uncorrected surfaces. One might wonder whether the relative energies found by a single CP correction are useful approximations to relative energies of structures found on the CP-corrected surface. Chart 3 bears on this question.

Table 2. Interatomic Distances for H-Bonding (Å)

structural feature	I	II	III	IV
−OH...O= (Turi)		1.702	1.788	1.899
−OH...O= (Y−T)		1.816	1.895	2.000
−OH...O= (CVH)		1.68	1.77	1.89
−CH...O= (Turi)			2.387	2.374
−CH...O= (Y−T)			2.493	2.538
−CH...O= (CVH)			2.34	2.39

structural feature	V		VI	VII	VIII
−OH...O< −OH...O= (Turi)	1.963; 1.975	−CH...O< −CH...O= (Turi)	2.535; 2.422	2.527	2.447
−OH...O<−OH...O= (Y−T)	2.078; 2.125	−CH...O< −CH...O= (Y−T)	2.641; 2.535	2.619	2.569
−OH...O< −OH...O= (CVH)	1.91; 1.98	−CH...O< −CH...O= (CVH)	2.50; 2.39	No data	2.43

The single point CP correction seems quite effective for all calculations with or without correlation both in small and larger basis sets, matching the net correction found on the CP surface very closely. Detailed data illustrating this point are in Table S2, Supporting Information. CVH report values of binding energies obtained by full CP corrections which are larger than the values obtained by single-point CP corrections. We confirm this observation.

New Equilibrium Dimeric Forms

We investigated some species not described previously. These include relative minima of the dimer which incorporate the formic acid fragment in a less stable cis (HCOH angle ca. 0°) form. These structures, shown in Table 1, are less stable than the analogs formed with all-trans formic acid, by about the 4−5 kcal/mol energy difference between cis and trans formaldehyde in the gas phase. One interesting form of this type is **III′** which has just been detected experimentally by Marushkevich et al.[16] who induced a trans-to-cis transition in **III** by infrared irradiation. **III′** is still more stable than all the trans−trans species bound only by CH.... O attractions. So is a cis−trans version **V′** of the low-energy species **V** with -H...OH...O< bonds. We also found a system with one conventional −OH...O= bond linking a **I**-cis acceptor with a **I**-trans donor acid, forming an open structure not otherwise stabilized, with the planes of the acids nearly orthogonal.

Geometric Parameters: Influence of the CP Corrections. Table S3 (Supporting Information) shows computed bond lengths for formic acid monomer **I** and Turi's set of dimers **II**−**VIII**. Turi's structures differ from ours in subtle ways in intramonomer C−H, C−O, and C=O distances, which we think are attributable to the differences in basis sets. Both sets of calculations faithfully represent the changes in lengths of OH bonds participating in H-bonding.

As Table 2 shows we predict larger −OH...O= and −OH...O−H bond lengths than Turi or CVH report, which we attribute to our systematic optimization of structures in the CP-corrected regime (in the first case) and perhaps to our superior basis set (in the second case). Turi explored the CP-corrected surface for species **II** and found that the −OH...O= distance increased by about 0.05 Å; our method produces an extension of about 0.1 Å. It appears that Turi made CP energy corrections for all other species at the minima of the noncorrected potentials.

Table 3. Selected Interatomic Distances for Cis−Trans Formic Acid Dimers (Å)

species H...A	III′	V′	Open trans-donor
−OH...O= −OH...O<	1.864	2.015	1.897
−CH...O=		2.055	
	2.384		

Geometry of New Structures. The intramolecular structural parameters of the new structures resulting from the association of one trans and one cis formic acid are unsurprising. Values are collected in the Supporting Information. The intermolecular distances shown in Table 3 suggest that the double role played by the OH group in **V′** (as in **V**) weakens the net attraction in these species. Conventional H-bonding is strongest in **II**, to judge from the short bond =O...HO− distance.

Reaction Paths

Considering the association path forming **II** from monomeric formic acid, BTYS[12] challenged the common notion that **II** forms by synchronous formation of its two hydrogen bonds. These investigators pointed out the statistical advantage of a two-step assembly of the stable species. On that basis one would expect that the association would proceed in at least two steps, as a first strong OH...O H-bond is formed, with the trans-formic acid fragments otherwise almost arbitrarily oriented. If two trans-formic acid monomers interact in this way, then the open form reverts without any apparent activation barrier to species **II** or **III**. When a single H-bond is formed between cis and trans formic acid, a metastable species is formed. It is stable with respect to two trans formic acid species by a mere 0.5 kcal/mol (ZPE corrected) but stable with respect to cis and trans formic acid molecules by about 5 kcal/mol. This open species can rearrange to **III** by cis−trans reversion of one formic acid fragment.

BTYS[12] located a local equilibrium structure which they termed "acyclic" and which appears to be species **III,** lying according to their calculations ca. 6 kcal/mol above **II** and isolated from **II** by an activation barrier they estimated to be ca. 3 kcal/mol. That is, the barrier from **II** to **III** is about 9 kcal/mol. We have re-examined the reaction path between **III** and the C_{2h} species **II**. Our estimate of interconversion barriers of 6.79 kcal/mol (**II** → **III**) and 2.25 kcal/mol (**III** → **II**) (Table 4) are lower than the values quoted by BTYS,[10]

Formic Acid Dimers

J. Chem. Theory Comput., Vol. 4, No. 3, 2008 **537**

Table 4. Energy (kcal/mol unless Otherwise Designated) and Selected Interatomic Distances (Å) of Transition States for Interconversions Leading to and from **II**[a]

species	V→II	III→II	Open→II
structure			
−OH...O= (Y−T)	1.9744, 4.4892	1.9634, 3.9118	2.0074, 2.1179
−OH...O= (BTYS)		1.847	
barrier from **II** (w. ZPE)	7.41 (6.37)	6.80 (5.76)	15.61 (13.85)
reverse barrier (w. ZPE)	1.41 (1.12)	2.26 (1.77)	5.08 (4.39)
E(hartrees)	−378.7348638	−378.7324325	−378.7183938
ZPE	43.856	43.759	43.033
barrier from **II** −SPCP (ZPE)	7.56 (6.64)	6.73 (5.74)	15.54 (13.93)
reverse barrier −SPCP (ZPE)	1.74 (1.55)	2.31 (1.84)	5.02 (4.36)

[a] The path linking the stable species **II** to the **Open** form is quite different from those leading from **III**, **IV**, or **V**. The **Open** form is a complex of a trans H-bond donor with a cis H-bond acceptor, so passage from the stable dimer **II** requires both partial H-bond breaking and trans−cis isomerization. This is why the activation energy on the order of the sum of the energy of a hydrogen bond added to the activation energy is required for trans−cis isomerization.

which once again we attribute to our use of the CP-corrected potential surface. Zero Point Energy differences reduce the barriers still further, to 5.76 and 1.77 kcal/mol respectively.

We have also established a path connecting the species **V** with **II**. Reversion of **V** to **II** is opposed by only about 1 kcal/mol. The energy and structure of the **V**→**II** and **III**→**II** transition states are very similar, though they are distinct at the convergence tolerance imposed in the transition state search. It would seem reasonable to consider the paths to traverse a rather flat upland or mesa rather than the more familiar picture of a high-curvature mountain pass. Our efforts to find a transition state for the passage of **IV** to **II** or **III** have not been successful.

Vibrational Spectra of Formic Acid Species

Irradiation of formic acid vapor with 3000 cm^{-1} light can produce any species which has an activation barrier less than about 8 kcal/mol from species **II**. The possibility that either **III** or **V** is accessible by IR excitation of **II** suggests that we should try to distinguish these species by their vibrational spectra. The absorption in the region of the OH stretch is sufficiently noisy that we should look elsewhere. In following sections we will establish reliability of our computations of harmonic and anharmonic vibrational frequencies and explore the possibility of fingerprinting the low-lying species.

Vibrations I: The Cis and Trans Monomers. First we establish the accuracy of the level of calculation we have chosen. Table 5 contains values for trans-formic acid (trans-**I**) frequencies with and without Barone anharmonicity estimates[17] as incorporated in Gaussian03. The anharmonic frequencies obtained by Barone's method agree remarkably well with most FTIR values. While OH and CH stretches are overestimated by 40 and 80 wave numbers respectively, the other modes all agree within 10 wave numbers.

We can distinguish the *cis* from *trans* computed spectra in the fingerprint region 600 to 670 cm^{-1} by the doublet at about 620 and 640 cm^{-1} computed for the more stable trans form and shown in Chart 4, the schematic representation of the experimental and computed spectra. The less stable cis form displays only a single absorption, well to the blue of this feature. The strong absorption of the OH out-of-plane motion lies very low (ca. 500 cm^{-1}). No such simple discriminating feature of the spectrum is available in the

**Table 5.** Fundamental Vibrational Frequencies for Cis and Trans Formic (cm^{-1})[a]

MODE	cis		trans		
	HARM	ANHARM	HARM	ANHARM	EXP[18]
1 OH str	3862.5	3674.6	3797.0	3607.4	3568.0
2 CH str	3035.4	2894.3	3132.0	3020.9	2938.7
3 C=O str	1845.4	1810.81	1807.4	1774.2	1775.5
4 OCH bend	1447.2	1412.1	1428.8	1401.2	1393.5
5 COH bend	1293.5	1248.5	1311.7	1222.4	1216.6
6 CO str	1117.4	1089.9	1143.2	1109.8	1105.5
7 OCO bend	**658.5**	**651.9**	**633.3**	**626.2**	**620.0**
8 CH oop	1042.5	1020.2	1064.2	1041.3	1033.3
9 OH oop	**511.2**	**480.2**	**670.8**	**638.3**	**641.8**

[a] Frequencies in wave numbers for formic acid computed in MP2/6-311+G(d,p) with Barone anharmonicity corrections. Modes 1−7 are in-plane motions, and modes 8 and 9 are out-of-plane motions ("oop"). Intense transitions are in bold face. The primary distinction between cis and trans isomers' spectra is in the splitting of the intense transitions 7 and 9.

region from 1000 to 1300 cm^{-1} although the computed frequencies for the trans isomer are consistently closer to the observed absorptions.

Vibrations II: Calibration with the Water Dimer. Water dimer is one of the most thoroughly studied hydrogen-bonded systems, so we wished to use the system as a reference point and to establish expectations for the methods we use. Table 6 shows separately the effect of CP corrections and Barone anharmonicity estimates (as implemented in Gaussian03) on the values of vibrational frequencies. The reported harmonic values listed in the table are not scaled, but if the MP2 factor 0.946 is applied to the frequencies of the harmonic modes, the mean absolute deviation (MAD) is substantially improved from 100 to 43 wave numbers (no CP) or from 77 to 26 wave numbers (CP corrected).

We take note of the well tested vibrational self-consistent method of Chaban, Jung, and Gerber,[23] implemented in GAMESS software as VSCF. This method does extremely well for the intramolecular modes. The soft intermolecular modes, which have large displacements and serious inter-mode coupling are not realistically described in VSCF, and even the pairwise coupling introduced in a refined version called cc-VSCF does not yield satisfactory results for these

Chart 4. Distinguishing Feature of Trans vs Cis Formic Acid[a]

Schematic spectra for cis and trans formic acid
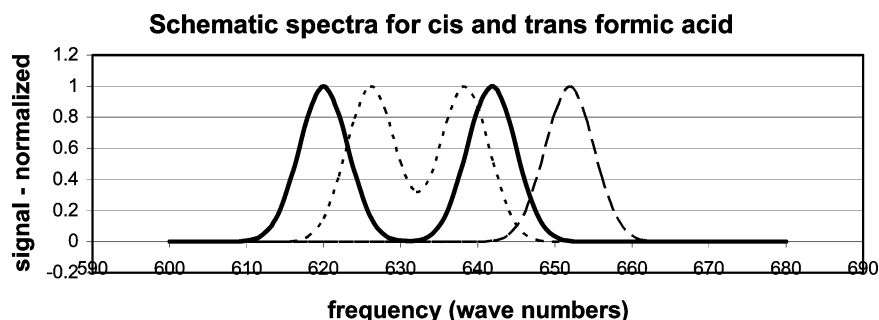
[a] Solid=experimental spectrum of formic acid showing a doublet centered at 630 cm^{-1} and split by about 30 cm^{-1}; dashed line=computed spectrum of the cis species showing an intense transition about 650 cm^{-1}; dotted line=computed spectrum for the trans species, showing a doublet centered at about 630 cm^{-1} and split by about 10 cm^{-1}. Computed values are the result of Barone's anharmonicity method in the MP2/6-311+G(d,p) model.

Table 6. Barone Anharmonicity Estimates of Frequencies for the Water Dimer, with and without Counterpoise Corrections (cm^{-1})

MP2/6-311+G(d,p)		MP2/6-311+G(d,p) CP				
harmonic	anharmonic	harmonic	anharmonic	**VSCF**	**Exp**	**mode**
133	75	114	56	545	88[a]	A″ PA-rotn
172	138	129	86	414	103[a]	A′ PA-rotn
178	131	155	119	259	108[a]	A″ PD rotn
204	**142**	**156**	**123**	451	**143[b]**	**A′ Diss**
382	286	307	268	550	311[c]	A′ H ‖
665	526	569	459	769	523[c]	A″ H ⊥
1640	1593	1636	1591	1565	1599[c]	A′ PA bend
1664	1604	1655	1603	1612	1616[c]	A′ PD bend
3808	3649	3826	3670	3560	3601[d]	A′ PD sstr
3875	3699	3880	3706	3689	3660[d]	A′PA sstr
3975	3798	3975	3797	3733	3735[d]	A′ PD astr
3989	3805	3995	3821	3763	3745[d]	A″ PA astr
101 (43 [e])	22	77 (26[e])	32	21[f], 285[g]		MAD

[a] Brayly et al.[19] supersonic molecular beam expansion. [b] Keutch et al.[20] supersonic molecular beam expansion. [c] Wuelfert et al.[21] CARS. [d] Huang and Miller[22] molecular beam depletion spectroscopy. [e] Scaled by 0.946 MP2 factor. [f] Intramolecular modes. [g] Intermolecular modes. Total VSCF MAD 153 cm^{-1}, cc-VSCF reduces the MAD values to 21 (intramolecular), 210 (intermolecular), and 115 (overall). PA=proton acceptor; PD=proton donor: sstr=symmetric stretch, astr=asymmetric stretch, H ‖ refers to motion of a H involved in OH...O< H-bonding moving parallel to the O−O axis; H ⊥ refers to motion perpendicular to that axis; diss refers to the dimer's dissociative motion.

difficult modes. This may be attributed to the extensive coupling among low frequency intermolecular modes as well as their severe anharmonicity.

Anharmonicity corrections by Barone's method make significant improvements, especially in the low-frequency intermolecular modes. The MAD is reduced from 101 to 22 cm^{-1} (with no CP) or from 77 to 32 cm^{-1} (with CP). As we noted for monomeric formic acid and water the Barone method does best for motions which are not simple O−H or C−H bond stretches. CP corrections shift most intermolecular frequencies to the red. Scaling CP corrected frequencies or making anharmonicity corrections to vibrations computed without CP shifts produce the most accurate estimates of the cluster's vibrational frequencies. Combining CP and anharmonicity corrections produces intermolecular mode frequencies overcorrected to the red and has little effect on the intramolecular modes.

Characterization of the Most Stable Formic Acid Dimer II. The C$_{2h}$-symmetric dimer has been studied experimentally by Bertie and Michaelian[24] who reported Raman spectra, by Marechal who described gas-phase FTIR data,[25] by Halupka and Sander who reported the IR absorp-

tion of matrix isolated species,[26] and by others who investigated specific regions of the spectrum. B3LYP/6-31G(d) calculations followed by Pulay's mode-specific scaling reproduces the experimental data with admirable accuracy (MAD = 15 cm^{-1}).[27] Our calculations include estimates of harmonic frequencies with and without systematic counterpoise corrections and also frequencies corrected for anharmonicity by the Barone's method (Table 7).

All values reported in Table 7 apart from the Pulay entries are unscaled. However if the harmonic values are scaled by the factor 0.946 suitable for MP2 values, then the MAD is reduced from 79 to 60 cm^{-1} for the frequencies obtained on the CP-corrected surface and from 66 to 40 cm^{-1} for the frequencies obtained without CP. The results suggest that one obtains the most reliable representation of the experimental spectrum with unscaled Barone anharmonic values obtained without counterpoise corrections. With a MAD of 21 cm^{-1}, these results come close to the Pulay-scaled values.

Scott and Radom's definition of scaling factors for specific model chemistries and different factors for high frequencies and low frequencies produces a MAD of 42 cm^{-1} for

Table 7. Frequencies for Formic Acid C$_{2h}$-Symmetric Dimer (cm^{-1})[e]

	MP2/6-311+G(d,p) - CP				MP2/6-311+G(d,p)	
A$_g$	Harmonic	Anharm	EXP[a–c]	Pulay Scaling[d]	harmonic	Anharm
1(1)	3457.3	3239.5	2949[c]	2968	3330.5	3079.2
2(1)	3144.1	2981.7	3035[c]	2946	3145.0	2970.2
3(1)	1748.9	1707.9	1670[c]	1671	1731.7	1691.6
4(1)	1462.6	1417.2	1415[c]	1409	1481.6	1419.6
5(1)	1400.4	1358.2	1375[c]	1366	1414.8	1337.4
6(1)	1235.8	1200.4	1214[c]	1284	1252.6	1217.3
7(1)	675.4	667.5	677[c]	663	683.9	674.6
8(1)	172.2	160.4		172	188.4	177.2
9(1)	149.3	138.7	137[c]	148	162.4	147.4
A$_u$						
10(1)	1097.6	1072.1	1050[c]	1061	1105.3	1078.7
11(1)	**917.1**	**867.3**	**942[a], 908[b], 917[c]**	**917**	**939.1**	**934.6**
12(1)	156.1	147.4	163[c]	159	162.4	157.6
13(1)	69.4	67.2	68[c]	66	60.7	66.6
B$_g$						
14(1)	1086.3	1062.0	1060[c]	1049	1084.4	1064.9
15(1)	885.9	821.3		843	922.1	873.2
16(1)	234.3	217.4	230[c]	237	229.3	230.7
B$_u$						
17(1)	**3517.1**	**3305.2**	**2992[a], 3000[b], 3000[c]**	**3072**	**3414.3**	**3173.1**
18(1)	**3141.5**	**2978.8**	**2950[a], 2944[b], 2957[c]**	**2957**	**3141.6**	**2969.8**
19(1)	**1795.5**	**1761.2**	**1728[a], 1740[b], 1754[c]**	**1752**	**1788.7**	**1751.8**
20(1)	1454.4	1411.6	1450[c]	1454	1460.3	1413.2
21(1)	1391.1	1347.8	1373[a], 1364[b], 1365[c]	1365	1404.8	1363.7
22(1)	**1241.7**	**1201.7**	**1226[a], 1215[b], 1218[c]**	**1218**	**1258.0**	**1226.9**
23(1)	689.5	678.9	712[a], 699[b], 697[c]	708	703.4	691.5
24(1)	213.0	198.0	248[c]	248	243.1	230.4
MAD	79	45		15	66	21
(scaled)	(60)				(40)	

[a] Ar matrix, Halupka and Sander, ref 13. [b] Gas-phase FTIR, Marechal, ref 12. [c] Raman from Bertie and Michaelian, ref 11. [d] Computations from Fernandez, Gomez Marigliano, and Varetti, ref 14. [e] Very intense transitions in IR are in bold. A$_g$ and B$_g$ absorptions are observed only in the Raman.

frequencies found without systematic CP correction. Omitting two outliers, the OH stretches, reduces MAD to 24 cm^{-1}.

A referee pointed out to us that experimental data and theoretical estimates for the vibrational frequencies of the C$_{2h}$-symmetric dimer of acetic acid were available[28,29] so we conducted MP2/6-311+G(d,p) calculations of the optimum structure with and without systematic CP corrections and the vibrational frequencies of the species including Barone estimates of anharmonicity corrections. Details are to be found in the Supporting Information. CP corrections reduce the estimated strength of intermolecular H-bonds and reduce the frequencies of relative motion of the monomers. For CP calculations the MAD in cm^{-1} for predicted frequencies relative to experimental values is 52 (unscaled) or 40 (scaled by the MP2 value, 0.953). For the structure optimized without CP corrections, the MAD in Barone estimates is 25 cm^{-1}. This value omits one serious outlier. Simple scaling of the harmonic values yields a comparable MAD.

Vibrational Fingerprinting of Dimeric Formic Acid Species. The C$_{2h}$-symmetric form **II** must be the dominant dimeric species in the gas phase, but irradiation may produce one or more of the low-lying isomers **III**, **IV**, and **V**. The presence of even rather small amounts of a less stable isomer can be verified by sufficiently sensitive vibrational spectrometry, so it is of interest to see if the less stable isomers

have characteristic absorptions which will aid in their detection. Tables S4 and S5 (Supporting Information) contain computed frequencies for low-energy species **III, IV,** and **V**, the harmonic values corrected for anharmonicity and obtained with and without CP corrections.

The C$_{2h}$ symmetry of some of formic acid's dimeric forms makes some transitions symmetry-forbidden. These weakly absorbing transitions are not suitable for fingerprinting. Frequencies of these transitions are parenthesized in Table 8. The lowest energy dimeric species (**II**) has a simple spectrum owing to its C$_{2h}$ symmetry. Where **II** has a single intense absorption for the OH out-of-plane motion at about 920 cm^{-1}, the three energy-accessible isomers **III, IV,** and **V** have distinctive OH out-of-plane frequency doublets, shifted to the red relative to the frequency of the analogous motion in **II**. The mean red shifts and splitting in the doublets may be useful as a fingerprint. Those motions which seem most promising as fingerprints are highlighted in Table 8. **IV** could be recognized by its enormous red shift, as shown in Table 9. **V** would have a smaller red shift and a small splitting. **III** is recognizable by its substantial red shift and the large splitting. Compared with **II,** the CO stretching doublets for less stable dimers **III, IV,** and **V** also have substantially lower frequency. These do not seem to be so helpful as the OH out-of-plane absorptions since they are

540 *J. Chem. Theory Comput., Vol. 4, No. 3, 2008*

Yavuz and Trindle

Table 8. Harmonic (A) and Anharmonic (B) Frequencies for Low Energy Species[a]

system	species **II**	species **III**	species **IV**	species **V**
		(A)		
frequencies				
OCO bend	689, (675)	670, 645	663, 632	671, 645
COH oop	**917, (884)**	**854, 692**	**792, 651**	**801, 723**
OCH oop	1097, (1086)	1097, 1079	1075, 1073	1076, 1064
CO str	*1241, (1235)*	*1205, 1170*	*1191, 1107*	*1188, 1143*
COH bend	1390, (1400)	1375, 1333	1366, 1288	1358, 1299

system	species **II**	species **III**	species **IV**	species **V**
		(B)		
frequencies				
OCO	679, (668)	660, 640	643, 621	678, 649
COH oop	**935, (821)**	**806, 639**	**692, 579**	**771, 664**
OCH oop	1072, (1062)	1063, 1051	1048, 1043	1052, 1041
CO str	*1227, (1200)*	*1168, 1135*	*1160, 1065*	*1157, 1106*
COH bend	1358, (1348)	1349, 1292	1328, 1240	1317, 1256

[a] Bold and italicized frequencies are candidates for fingerprints distinguishing Species **III**, **IV**, and **V** from **II**.

Table 9. OOH Out-of-Plane Shifts and Doublet Splitting (cm^{-1})

species	**III**	**IV**	**V**
mean red shift (harmonic)	144	195	155
splitting (harmonic)	158	163	78
mean red shift (anharmonic)	213	299	151
splitting (anharmonic)	167	141	88

not so easily distinguishable. The weakly absorbing COH in-plane bends are still less useful.

Recently Marushkevich et al.[30] have produced a dimer incorporating both a cis and a trans formic acid, which seems to be the species **III′**. This species lies about 8.8 kcal/mol above the most stable dimer **II**. Frequencies computed by these investigators and our comparable values computed with full CP are recorded in Table 10. There is a potential fingerprint in the OH out-of-plane motion and (less marked) in the CO doublet. The OH out-of-plane motion distinguishes the species, the splitting in the doublet being much larger in **III′** than **III**. The same pattern is displayed in the COH in-plane bends and the CO (single bond) stretches, but to a lesser degree.

Conclusions

We have revisited the dimers of trans formic acid defined by Turi (**II**−**VIII** in his designation). We used a consistent model chemistry, MP2/6-311+G(d,p) including zero-point-energy corrections and employing full counterpoise (CP) corrections in the optimizations and vibrational frequency calculations. Optimization with systematic CP corrections produces structures with longer and weaker hydrogen bonds than optimization without CP corrections. It is interesting to note that single point CP corrections produce binding energies almost identical with the binding energies obtained by systematic CP corrections.

In addition we have characterized several dimers containing one cis formic acid monomer and one trans monomer.

Table 10: Selected Harmonic Frequencies and Anharmonic Frequencies in cm^{-1} for Cis−Trans (**III′**) and Trans−Trans (**III**) Formic Acid Complexes[a]

	Harmonic Frequencies			
	species **III′**		species **III**	
modes	Y-T (full CP)	M et al	Y-T (full CP)	M et al
OCO	682, 674		670, 645	
COH out of plane	**899, 595**	946, 573	**854, 692**	936, 699
OCH out of plane	1071, 1069		1097, 1079	
CO stretch	*1204, 1139*	1213, 1153	*1205, 1170*	1205, 1156
COH in plane	1373, 1304		1333, 1375	

	Anharmonic Frequencies			
	species **III′**		species **III**	
modes	Y-T (no CP)	M et al	Y-T (no CP)	M et al
OCO	673, 668		660, 640	
COH out of plane	**874, 525**	946, 573	**806, 639**	936, 699
OCH out of plane	1060, 1052		1063, 1051	
CO stretch	*1184, 1128*	1213, 1153	*1168, 1135*	1205, 1156
COH in plane	1394, 1264		1349, 1292	

[a] Bold and italicized frequencies are candidates for fingerprints distinguishing species **III′** from **III**.

These are called **III′** (recently obtained experimentally) and **V′**. We also found a bound **Open** form with one conventional OH...O= bond but no secondary CH...O interaction. These species are all bound relative to two trans formic acid monomers. Any of the species **II**-**VII**, **III′**, and **V′** and **Open** may play a role in the association of formic acid monomers. **III**, **IV**, and **V** may appear in experiments in which formic acid vapor is irradiated with infrared photons. Our estimates of the activation barrier for the transformations **II**→**V** and **II**→**III** show that these conversions are energetically possible under such circumstances. We can say nothing definite about the passage of species **IV** to **II** or **III**.

The purpose of this study was to identify candidates for the "acyclic" form of the formic acid dimer inferred by Shipman et al. from pulse IR studies of formic acid vapor and to estimate possible characteristic infrared absorptions which could allow experimental identification of the intermediate. According to our estimates of harmonic and anharmonic frequencies, the OH out-of-plane motion and the CO stretches may serve to identify which of the accessible species **III, IV,** and **V** are produced in irradiation experiments.

Formic Acid Dimers

J. Chem. Theory Comput., Vol. 4, No. 3, 2008 **541**

Supporting Information Available: Numerous tables of structures and frequencies and Gaussian log files for all systems. This material is available free of charge via the Internet at http://pubs.acs.org.

References

(1) All ZPE corrections obtained by unscaled harmonic frequencies. Use of the ZPE scaling suggested by Scott and Radom (ref 2) or use of anharmonic frequencies has little impact on the ΔZPE values.

(2) Scott, A. P.; Radom, L. *J. Phys. Chem.* **1996**, *100*, 16502.

(3) The convention for *trans* and *cis* nomenclature agrees with Brinkmann et. al. [ref 14] and most other investigators.

(4) Tsuzuki, S.; Uchimaru, T.; Matsumura, K.; Mikami, M.; Tanabe, K. *J. Chem. Phys.* **1999**, *110*, 11906.

(5) Matylitsky, V. V.; Riehn, C.; Gelin, M. F.; Brutschy, B. *J. Chem. Phys.* **2003**, *119*, 10553.

(6) Luckhaus, D. *J. Phys. Chem. A* **2006**, *110*, 3151.

(7) Shipman, S. T.; Douglass, P. C.; Yoo, H. S.; Hinkle, C. E.; Mierzejewski, E. L.; Pate, B. H. *Phys. Chem. Chem. Phys.* **2007**, *9*, 4572.

(8) Winkler, A.; Mehl, J. B.; Hess, P. *J. Chem. Phys.* **1993**, *100*, 2717.

(9) Boys, S. F.; Bernardi, F. *Mol. Phys.* **1970**, *19*, 553.

(10) Simon, S.; Duran, M.; Dannenberg, J. J. *J. Chem. Phys.* **1996**, *105*, 11024.

(11) Turi, L. *J. Phys. Chem.* **1996**, *100*, 11285.

(12) Qian, W.; Krimm, S. *J. Phys. Chem. A* **2001**, *105*, 5046.

(13) Chocholoušová, J.; Vacek, J.; Hobza, P. *Phys. Chem. Chem. Phys.* **2002**, *4*, 2119.

(14) Frisch, M. J.; Trucks, G. W.; Schlegel, H. B.; Scuseria, G. E.; Robb, M. A.; Cheeseman, J. R.; Montgomery, J. A., Jr.; Vreven, T.; Kudin, K. N.; Burant, J. C.; Millam, J. M.; Iyengar, S. S.; Tomasi, J.; Barone, V.; Mennucci, B.; Cossi, M.; Scalmani, G.; Rega, N.; Petersson, G. A.; Nakatsuji, H.; Hada, M.; Ehara, M.; Toyota, K.; Fukuda, R.; Hasegawa, J.; Ishida, M.; Nakajima, T.; Honda, Y.; Kitao, O.; Nakai, H.; Klene, M.; Li, X.; Knox, J. E.; Hratchian, H. P.; Cross, J. B.; Bakken, V.; Adamo, C.; Jaramillo, J.; Gomperts, R.; Stratmann, R. E.; Yazyev, O.; Austin, A. J.; Cammi, R.; Pomelli, C.; Ochterski, J. W.; Ayala, P. Y.; Morokuma, K.; Voth, G. A.; Salvador, P.; Dannenberg, J. J.; Zakrzewski, V. G.; Dapprich, S.; Daniels, A. D.; Strain, M. C.; Farkas, O.; Malick, D. K.; Rabuck, A. D.; Raghavachari, K.; Foresman, J. B.; Ortiz, J. V.; Cui, Q.; Baboul, A. G.; Clifford, S.; Cioslowski, J.; Stefanov, B. B.; Liu, G.; Liashenko, A.; Piskorz, P.; Komaromi, I.; Martin, R. L.; Fox, D. J.; Keith, T.; Al-Laham, M. A.; Peng, C. Y.; Nanayakkara, A.; Challacombe, M.; Gill, P. M. W.; Johnson, B.; Chen, W.; Wong, M. W.; Gonzalez, C.; Pople, J. A. *Gaussian 03, Revision C.02*; Gaussian, Inc., Wallingford, CT, 2004.

(15) Brinkmann, N. R.; Tschumper, G. S.; Yan, G.; Schaefer, H. F. *J. Phys. Chem. A* **2003**, *107*, 10208.

(16) Marushkevich, K.; Khriachtechev, l.; Lundell, J.; Räsänen, M. *J. Am. Chem. Soc.* **2006**, *128*, 12060.

(17) Barone, V. *J. Chem. Phys.* **2005** *122*, 014108. Barone, V. *J. Chem. Phys.* **2004**, *120*, 3059.

(18) Luiz, G. M. R. S.; Scalabrin, A.; Pereira, D. *Infrared Phys. Technol.* **1997**, *38*, 45

(19) Braly, L. B.; Liu, K.; Brown, M. G.; Keutsch, F. N.; Fellers, R. S.; Saykally, R. J. *J. Chem. Phys.* **2000**, *112*, 10314.

(20) Keutsch, F. N.; Braly, L. B.; Brown, M. G.; Harker, H. A.; Petersen, P. B.; Leforestier, C.; Saykally, R. J. *J. Chem. Phys.* **2003**, *119*, 8927.

(21) Wuelfert, S.; Herren, D.; Leutwyler, S. *J. Chem. Phys.* **1987**, *86*, 3751.

(22) Huang, Z. S.; Miller, R. E. *J. Chem. Phys.* **1989**, *91*, 6613.

(23) Chaban, G. M.; Jung, J. O.; Gerber, R. B. *J. Chem. Phys.* **1999**, *111*, 1823.

(24) Bertie, J. E.; Michaelian, K. H. *J. Chem. Phys.* **1982**, *76* 886

(25) Marechal, Y. *J. Chem. Phys.* **1987**, *87*, 6344.

(26) Halupka, M.; Sander, M. *Spectrochim. Acta, Part A* **1998**, *54*, 495.

(27) Fernandez, L. E.; Gomez Marigliano, A. C.; Varetti, E. L. *Vibr. Spectrosc.* **2005** *37* 179

(28) Turi, L.; Danneberg, J. J. *J. Phys. Chem.* **1993**, 97 12197

(29) Dreyer, J. *J. Chem. Phys.* **2005**, *122*, 184306.

(30) Marushkevich, K.; Khriachtechev, l.; Lundell, J.; Räsänen, M. *J. Am. Chem. Soc.* **2006** *128*.